ELSEVIER

Journal of Organometallic Chemistry 626 (2001) 161–167

Journal of Organometallic Chemistry

www.elsevier.nl/locate/jorganchem

The behaviour of polydentate hydrazonic ligands derived from 2-acetylpyridine towards organotin compounds☆ Part II. The monoorganotin(IV) complexes

Mauro Carcelli [a,*], Andrea Fochi [a], Paolo Pelagatti [a], Giancarlo Pelizzi [a], Umberto Russo [b]

[a] *Dipartimento di Chimica Generale ed Inorganica, Chimica Analitica, Chimica Fisica, Università degli Studi di Parma, Parco Area delle Scienze 17/A, 43100 Parma, Italy*

[b] *Dipartimento di Chimica Inorganica, Metallorganica e Analitica, Università di Padova, Via Loredan 4, 35131 Padova, Italy*

Received 14 November 2000; accepted 8 January 2001

Abstract

The study of the reactivity of the ligands bis(2-acetylpyridine)thiocarbonohydrazone (**H_2apt**), 2-acetylpyridine thiosemicarbazone (**Hapts**) and 2-acetylpyridine semicarbazone (**Haps**) towards monoorganotin(IV) compounds was carried out; all the new derivatives were spectroscopically (IR, ^{1}H-NMR and Mössbauer) characterised. The X-ray crystal structures of [(*n*-Bu)Sn(**Hapt**)Cl_2]·1.5H_2O, [PhSn(**Hapt**)Cl_2]·C_2H_5OH·H_2O and [PhSn(**aps**)Cl_2] were reported and a comparison was made with the already characterised diorganotin complexes of the same ligands.

Keywords: Organotin compounds; Polydentate ligands; Sulphur ligands; Pyridyl ligands

1. Introduction

Much work has been carried out on the coordination chemistry and the biological effects of 2-pyridyl thiosemicarbazones and of their transition metal complexes [2], whereas a lot less is known about the interaction between them and organotin compounds [3–7]. Recently, the structurally related 2-pyridyl thiocarbonohydrazones [8] and their complexes [9,10] also attract some attention. In the context of our continuous interest for the structural and biological properties of organotin compounds [11], we started the study of the coordination behaviour of bis(2-acetylpyridine)-thiocarbonohydrazone (**H_2apt**), 2-acetylpyridine thiosemicarbazone (**Hapts**) and, for comparison, 2-acetylpyridine semicarbazone (**Haps**) (Scheme 1), towards transition metals [10,12] and diorganotin [1]. Here we report the synthesis and characterisation of butyl and phenyl monoorganotin complexes of the above ligands; the X-ray crystal structures of [(*n*-Bu)Sn(**Hapt**)Cl_2]·1.5H_2O, [PhSn(**Hapt**)Cl_2]·C_2H_5OH·H_2O and [PhSn(**aps**)Cl_2] are also discussed.

2. Experimental

2.1. Materials and methods

All reagents were of commercial quality and used without further purification. Elemental analyses (C, H, N and S) were carried out on an automatic Carlo Erba CHNS-O EA1108 elemental analyser. Infrared spectra (4000–400 cm^{-1}) for KBr discs were recorded on a Nicolet 5PC FT-IR spectrometer, the mass spectra (CI) on a Finnigan SSQ710 instrument, ^{1}H-NMR spectra on a Bruker ACX 300 instrument at room temperature (r.t.); chemical shifts (δ) are given in ppm referenced to internal tetramethylsilane. Melting points were obtained with a Gallenkamp MFB-595 apparatus in open capillaries.

Mössbauer spectra were collected in an Air Liquide variable temperature cryostat at 80 K. The $Ca^{119}SnO_3$

☆ For Part I, see Ref. [1].

* Corresponding author.

E-mail address: carcelli@unipr.it (M. Carcelli).

0022-328X/01/$ - see front matter
PII: S0022-328X(01)00677-5

source (nominal strength 15 mCi, New England Nuclear) was kept at r.t. and moved at constant acceleration with a triangular wave form. Suitable computer programs were employed in the fitting procedure of the experimental spectra to Lorentzian line shapes by using least-squares computer minimisation techniques. The isomer shift data are relative to r.t. $CaSnO_3$.

X-ray data collection, structure determination and refinement of compounds ***1***$\cdot 1.5H_2O$, ***2***$\cdot C_2H_5OH\cdot H_2O$ *and* ***6***. Air stable crystals suitable for structural determination by single crystal X-ray diffraction were obtained for compounds **1**$\cdot 1.5H_2O$, **2**$\cdot C_2H_5OH\cdot H_2O$ and **6**. Details about X-ray experimental conditions, data collection and refinement are given in Table 1. The collected data were corrected for Lorentz and polarisation effects; compounds **1**$\cdot 1.5H_2O$ and **2**$\cdot C_2H_5OH\cdot H_2O$ were also corrected for absorption according to Walker and Stuart [13]. Compound **6** was corrected for absorption employing the SADABS [14] program. None of the compounds showed signs of decay through the collection procedure. The phase problem for all the compounds was solved by direct methods. Structure refinement was obtained by full-matrix least squares based on F^2. All non-hydrogen atoms were refined anisotropically. Only part of the hydrogen atoms were located in the Fourier maps, the remaining ones were put in calculated positions and constrained to ride on their carrying atoms. Hydrogen atoms of water, wherever present as the crystallisation solvent, were ignored. Calculations were performed on an ENCORE91 computer and a PIII personal computer, using the following program packages: SIR92 [15], SHELXL97 [16], PARST [17], ORTEP3 [18] and SAINT [19] for **6** only.

2.2. Syntheses

The ligands are prepared by standard methods [1].

[(n-Bu)Sn(Hapt)Cl$_2$*]*$\cdot 2H_2O$. (**1**$\cdot 2H_2O$) 0.1 g (3.2 mmol) of the ligand, dissolved in hot methanol (60 ml), and an equimolar amount of $BuSnCl_3$ (0.18 g) are refluxed for 2 h; the solution becomes deep yellow. **1**$\cdot 2H_2O$ precipitates by slow evaporation of the solution at r.t. Yield 48%; m.p. 242°C (dec.). Anal. Found: C, 38.30; H, 4.62; N, 14.51; S, 5.23. Calc. for $C_{19}H_{28}Cl_2N_6O_2SSn$: C, 38.41; H, 4.75; N, 14.14; S, 5.40%. ^{1}H-NMR ($CDCl_3$) δ_H: 1.03 (t, 3H, CH_3CH_2), 1.56 (m, 2H, CH_3CH_2), 1.99 (m, 2H, CH_2), 2.26 (t, 2H, $SnCH_2$), 2.41 (s, 3H, CH_3), 2.77 (s, 3H, CH_3), 7.26–8.66 (8H, $CH_{ar.}$), 9.19 (s, 1H, NH). X-ray diffraction quality crystals of **1**$\cdot 1.5H_2O$ are obtained by recrystallisation from heptane–ethanol.

Compounds **2**–**6** are prepared by using a similar procedure.

[PhSn(Hapt)Cl$_2$*]*$\cdot C_2H_5OH$. (**2**$\cdot C_2H_5OH$) Yield 65%; m.p. 250°C (dec.). Anal. Found: C, 44.20; H, 4.80; N, 13.36; S, 5.03. Calc. for $C_{23}H_{26}Cl_2N_6OSSn$: C, 44.26; H, 4.20; N, 13.46; S, 5.14%. ^{1}H-NMR (DMSO-d_6) δ_H: 2.59 (s, 3H, CH_3), 2.99 (s, 3H, CH_3), 7.40–8.60 (8H, $CH_{ar.}$), 11.77 (s, 1H, NH). Crystals of **2**$\cdot C_2H_5OH\cdot H_2O$ suitable for X-ray analysis are obtained by recrystallisation from ethanol.

[(n-Bu)Sn(apts)Cl$_2$*]*. (**3**) Yield 40%; m.p. 263°C (dec.). Anal. Found: C, 32.55; H, 4.19; N, 12.48; S, 7.35. Calc. for $C_{12}H_{18}Cl_2N_4SSn$: C, 32.76; H, 4.12; N, 12.73; S, 7.29%. ^{1}H-NMR ($CDCl_3$) δ_H: 0.99 (t, 3H, CH_3CH_2), 1.53 (m, 2H, CH_3CH_2), 1.94 (m, 2H, CH_2), 2.22 (t, 2H, $SnCH_2$), 2.73 (s, 3H, CH_3), 5.74 (s, 2H, NH_2), 7.71 (t, 1H, H2), 7.97 (d, 1H, H4), 8.19 (t, 1H, H3), 8.63 (d, 1H, H1).

[PhSn(apts)Cl$_2$*]*. (**4**) Yield 50%; m.p. 245°C (dec.). Anal. Found: C, 36.30; H, 3.89; N, 12.67; S, 7.24. Calc. for $C_{14}H_{14}Cl_2N_4SSn$: C, 36.56; H, 3.07; N, 12.18; S, 6.97%. ^{1}H-NMR ($CDCl_3$) δ_H: 2.75 (s, 3H, CH_3), 7.50–7.61 (m, 5H, $CH_{phenyl} + NH_2$), 7.82 (t, 1H, H2), 8.16 (d, 2H, CH_{phenyl}), 8.34–8.44 (m, 3H, H1, H3, H4).

[(n-Bu)Sn(aps)Cl$_2$*]*$\cdot 3H_2O$. (**5**$\cdot 3H_2O$) Yield 70%; m.p. 218°C (dec.). Anal. Found: C, 30.07; H, 4.89; N, 11.67. Calc. for $C_{12}H_{24}Cl_2N_4O_4Sn$: C, 30.16; H, 5.04; N, 11.72%. ^{1}H-NMR ($CDCl_3$) δ_H: 0.98 (t, 3H, CH_3CH_2), 1.55 (m, 2H, CH_3CH_2), 1.97 (m, 2H, CH_2), 2.21 (t, 2H, $SnCH_2$), 2.59 (s, 3H, CH_3), 5.33 (s, 2H, NH_2), 7.64 (t, 1H, H2), 7.86 (d, 1H, H4), 8.15 (t, 1H, H3), 8.51 (d, 1H, H1).

[PhSn(aps)Cl$_2$*]*$\cdot 2.5H_2O$. (**6**$\cdot 2.5\ H_2O$) Yield 65%; m.p. 220°C (dec.). Anal. Found: C, 34.04; H, 4.07; N, 11.46. Calc. for $C_{14}H_{19}Cl_2N_4O_{3.5}Sn$: C, 34.39; H, 3.92; N, 11.46%. ^{1}H-NMR (DMSO-d_6) δ_H: 2.58 (s, 3H, CH_3), 7.52–7.68 (m, 5H, $CH_{phenyl} + NH_2$), 7.45 (t, 1H, H2), 8.16 (d, 2H, CH_{phenyl}), 8.22–8.24 (m, 2H, H1 + H4), 8.39 (t, 1H, H3). Crystals of **6** suitable for X-ray analysis are obtained by recrystallisation from toluene.

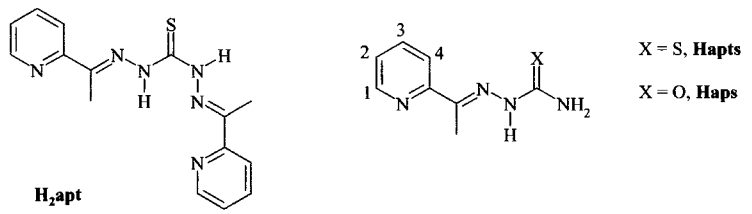

Scheme 1.

Table 1
Crystal data and structure refinement

Compound	**1**·1.5 H_2O	**2**·C_2H_5OH·H_2O	**6**
Empirical formula	$C_{19}H_{27}Cl_2N_6O_{1.5}SSn$	$C_{23}H_{28}Cl_2N_6O_2SSn$	$C_{14}H_{14}Cl_2N_4OSn$
Formula weight	585.16	642.21	443.88
Temperature (K)	293(2)	293(2)	293(2)
Diffractometer	Philips PW1100	Philips PW1100	Siemens SMART AXS1000
Data collection method	$\theta/2\theta$	$\theta/2\theta$	ω scan (hemisphere)
Number of frames			1235
Detector distance (cm)			5.000
Wavelength (Å)	0.71069	0.71069	0.71069
Crystal system	Monoclinic	Monoclinic	Monoclinic
Space group	$C2/c$	$C2/c$	$P2_1/c$
Unit cell dimensions			
a (Å)	25.341(6)	35.95(2)	8.920(3)
b (Å)	20.491(5)	8.894(5)	13.010(4)
c (Å)	10.020(3)	18.251(10)	14.426(4)
β (°)	99.28(2)	100.87(2)	91.55(1)
Volume (Å^3)	5135(2)	5731(6)	1673.5(9)
Z	8	8	4
Absorption coefficient (mm^{-1})	1.308	1.181	1.850
Crystal colour	red	orange	pale yellow
Crystal size (mm^3)	$0.6\times0.4\times0.3$	$0.45\times0.4\times0.3$	$0.3\times0.3\times0.25$
Theta range (°)	2.54–27.00	3.21–30.00	2.11–28.04
Reflections collected	5912	8585	9632
Independent reflections	5599 [R(int) = 0.0797]	8357 [R(int) = 0.0444]	3698 [R(int) = 0.0197]
Obs. reflections [$I>2\sigma(I)$]	1560	3514	3168
Completeness to theta (%)	99.9	99.8	91.1
Refinement method	Full-matrix least-squares on F^2	Full-matrix least-squares on F^2	Full-matrix least-squares on F^2
Data/restraints/parameters	5599/45/287	8357/0/327	3698/0/255
Goodness-of-fit on F^2	1.131	1.456	0.904
Final R indices [$I>2\sigma$(I)]	$R_1 = 0.0590$, w$R_2 = 0.1471$	$R_1 = 0.0531$, w$R_2 = 0.1363$	$R_1 = 0.0208$, w$R_2 = 0.0541$
R indices (all data)	$R_1 = 0.3150$, w$R_2 = 0.2825$	$R_1 = 0.2552$, w$R_2 = 0.2772$	$R_1 = 0.0268$, w$R_2 = 0.0570$
Largest difference peak and hole (e Å^{-3})	0.718 and −0.793	2.091 and −1.887	0.241 and −0.543

The reaction between **Haps** and Ph_2SnCl_2 in methanol gives rise to a mixture consisting of both **Haps** × HCl and **6**.

3. Results and discussion

The ligands react with butyl and phenyltin trichloride, despite the fact that they are *NN′O* or *NN′S* donors, giving the complexes **1**–**6** (Eq. (1)). **H_2apt** is able to give bimetallic complexes with transition metals [12], but it was not possible to obtain analogous compounds with organotin, even though the metal to ligand ratio was risen until 4:1 or $(C_2H_5)_3N$ was used to neutralise the hydrochloric acid resulting from the complexation and to deprotonate the ligand.

$$H_nL + RSnCl_3 = RSn(H_{n-1}L)Cl_2 + HCl \qquad \begin{matrix} n=1 & \text{Haps, Hapts} \\ n=2 & H_2\text{apt} \\ R = n\text{-Bu, Ph} \end{matrix} \qquad (1)$$

The ^{1}H-NMR spectra of the tin derivatives show some interesting features. In the pyridine ring, the resonance of the hydrogens follows the sequence H1, H4, H3, H2 in the free ligand (see Scheme 1 for the numbering order), but it is H1, H3, H4, H2 in **1**, **3**, and **5**. H1 is more deshielded in the diorganotin [1] than in the monoorganotin compounds; this is related to the atom which, besides the terdentate ligand, occupies the equatorial plane: in **1**, **3** and **5** there is the carbon atom of the organic group linked to tin, while in the diorganotin there is the more electronegative oxygen of the acetate group ([(n-Bu)$_2$Sn(**Hapt**)(OAc)], [(n-Bu)$_2$Sn(**apts**)(OAc)], [(n-Bu)$_2$Sn(**aps**)(OAc)]) or the chloride anion ([Ph_2Sn(**Hapt**)Cl]·H_2O) [1].

In the **2**, **4**, and **6** derivatives, the order of the pyridine hydrogens is significantly different (H3, H1, H4, and H2), because the proton H1 is under the influence of the ring current of the phenyl ring linked to tin: as shown by X-ray analysis, the distance between H1 and the centre of the phenyl ring is 3.36 Å in **6** and 3.64 Å in **2**.

The complex **6** is not stable in solution towards hydrolysis; by ^{1}H-NMR it is possible to follow the formation of free ligand, when deuterium oxide is added to its DMSO-d_6 solution. In the ^{1}H-NMR spec-

tra of **3** and **5** the NH_2 protons become magnetically equivalent and give a broad peak, as already noted elsewhere [1,20].

In the IR spectra of the complexes **3**–**6,** the deprotonation of the ligand is reflected by the absence of the ν(N–H) band; in the spectra of **5** and **6,** the ν(C=O) band is absent, too.

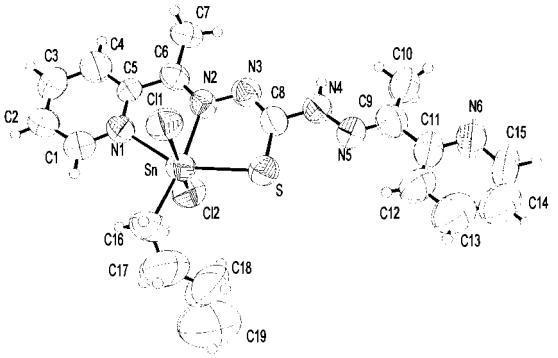

Fig. 1. Perspective view of compound **1**·1.5 H_2O with thermal ellipsoids at 50% probability level. The crystallisation water molecules are omitted.

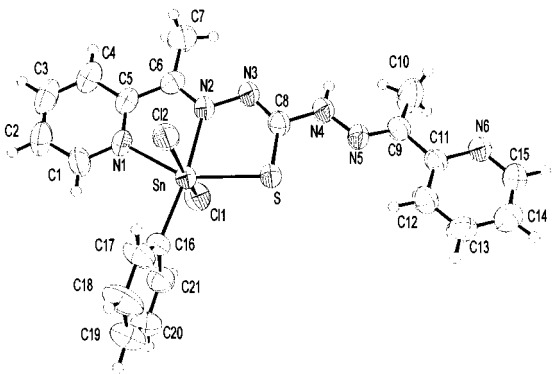

Fig. 2. Perspective view of compound **2**·C_2H_5OH·H_2O with thermal ellipsoids at 50% probability level. The crystallisation solvent molecules are omitted.

Table 2
Selected bond lengths (Å) and angles (°) for **1**·1.5H_2O

Sn–C16	2.13(1)	C16–Sn–N2	172.2(6)
Sn–N2	2.20(1)	C16–Sn–N1	101.4(6)
Sn–N1	2.29(1)	N2–Sn–N1	71.1(4)
Sn–Cl2	2.486(4)	C16–Sn–Cl2	97.3(5)
Sn–S	2.493(4)	N2–Sn–Cl2	84.7(3)
Sn–Cl1	2.551(4)	N1–Sn–Cl2	85.9(3)
S–C8	1.72(1)	C16–Sn–S	108.8(5)
N3–C8	1.33(1)	N2–Sn–S	78.6(3)
N3–N2	1.35(1)	N1–Sn–S	149.6(3)
N2–C6	1.31(1)	Cl2–Sn–S	93.9(1)
N4–C8	1.36(2)	C16–Sn–Cl1	90.4(5)
N1–C5	1.31(2)	N2–Sn–Cl1	86.5(3)
C6–C5	1.44(2)	N1–Sn–Cl1	83.9(3)
		Cl2–Sn–Cl1	168.3(1)
		S–Sn–Cl1	91.9(1)

Table 3
Selected bond lengths (Å) and angles (°) for **2**·C_2H_5OH·H_2O

Sn–C16	2.150(8)	C16–Sn–N2	172.2(3)
Sn–N2	2.226(7)	C16–Sn–N1	100.3(3)
Sn–N1	2.237(7)	N2–Sn–N1	72.0(3)
Sn–Cl1	2.476(3)	C16–Sn–Cl1	95.1(2)
Sn–S	2.481(2)	N2–Sn–Cl1	83.0(2)
Sn–Cl2	2.507(2)	N1–Sn–Cl1	86.4 (2)
S–C8	1.742(8)	C16–Sn–S	108.6(2)
N1–C5	1.35(1)	N2–Sn–S	79.1 (2)
N2–C6	1.30(1)	N1–Sn–S	151.0(2)
N2–N3	1.374(9)	Cl1–Sn–S	93.32(9)
N3–C8	1.33(1)	C16–Sn–Cl2	95.6(2)
N4–C8	1.36(1)	N2–Sn–Cl2	85.2(2)
C5–C6	1.46(1)	N1–Sn–Cl2	82.7(2)
		Cl1–Sn–Cl2	166.02(9)
		S–Sn–Cl2	91.89(8)

The coordination has been unequivocally established by means of the X-ray diffraction analysis of **1**·1.5 H_2O, **2**·C_2H_5OH·H_2O and **6**; Figs. 1 and 2 show the ORTEP diagrams and the atomic numbering schemes of the complex molecules in **1**·1.5H_2O and **2**·C_2H_5OH·H_2O, respectively. Selected bond angles and distances are shown in Tables 2 and 3. The two complexes show no significant differences other than the presence of a butyl group instead of a phenyl one in the coordination sphere of tin. In both compounds the ligand is monodeprotonated and acts as a terdentate *NN′S* donor; the coordination induces the formation of two five-membered chelate rings. In both compounds the SnNCCN ring is strictly planar, while the SnSCNN ring is planar within 0.08 Å. Two chlorine atoms in the axial positions and the phenyl or butyl group in the equatorial site complete the highly distorted octahedron. The distortion is mainly due to the stereochemical constraints imposed by the terdentate ligand, as shown by the N1–Sn–S angle largely different from the theoretic 180° value (149.6(3) for **1** and 151.0(2)° for **2**); for the same reason the N1–Sn–N2 and N2–Sn–S angles are considerably smaller than the expected 90°. The distortion can also be observed through the Cl1–Sn–Cl2 angle (166.8(1) and 168.5(1)°, respectively).

It is interesting to compare **1** and **2** with the previously characterised diorganotin complexes ([Ph_2Sn(**Hapt**)Cl] [1], [$(CH_3)_2$Sn(**apts**)Cl] [5] and [$(CH_3)_2$Sn(**apts**)(CH_3COO)]·CH_3COOH [6]) and with the trichloro complex [Sn(**fpt**)Cl_3] (**Hfpt**, 2-formylpyridine thiosemicarbazone) [4]. It can be noticed that in the monoorganotin complexes the N(pyridine)–Sn and N(imine)–Sn distances are shorter than in the diorganotin ones (N(pyridine)–Sn: 2.29(1) in **1**, 2.237(7) in **2** versus 2.509(8) in [Ph_2Sn(**Hapt**)Cl], 2.561(4) in [$(CH_3)_2$Sn(**apts**)(CH_3COO)]·CH_3COOH and even 2.688 Å in [$(CH_3)_2$Sn(**apts**)Cl]; N(imine)–Sn: 2.20(1), 2.226(7) versus 2.331(5), 2.431(4) and 2.359(4) Å, respectively); on the contrary, the Sn–S distance remains approxi-

mately unchanged (2.493(4), 2.481(2)–2.505(2), 2.509(1) and 2.478(2) Å). The shortest distances are in [Sn(**fpt**)Cl_3] (N(pyridine)–Sn 2.225(3), N(imine)–Sn 2.194(2), Sn–S 2.463(1) Å). It seems reasonable to conclude that when the Lewis acidity of the tin cation is higher, the metal–nitrogen distances are shorter. However, the crystal packing effects may play a relevant and difficult to rationalise role, as in [(n-Bu)$_2$Sn(**apts**)-(CH_3COO)] [1], where in the unit-cell there are two crystallographically independent molecules with significantly different tin–donor atom distances (N(pyridine)–Sn 2.383(5) and 2.445(4), N(imine)–Sn 2.367(4) and 2.370(4), Sn–S 2.641(2) and 2.582(2) Å).

In **1** and **2** the two *trans*- chlorine atoms show a slightly asymmetrical behaviour as evidenced by the Sn–Cl distances. The C–S distance is slightly longer than in free hydrazone. The hydrazone molecule is not strictly planar and can be described by two mean planes, one containing the coordination moiety and the other containing the free pyridine ring, C9, N5 and N4. The angles they form are about 6 and 10°, respectively. As already found in analogous complexes [1], upon complexation the ligand rearranges from the E–Z to the E–E form.

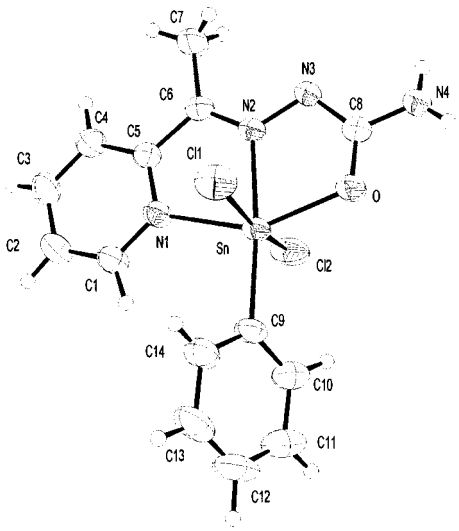

Fig. 3. Perspective view of compound **6** with thermal ellipsoids at 50% probability level.

Table 4
Selected bond lengths (Å) and angles (°) for **6**

Sn–O	2.099(2)	O–Sn–C9	112.30(7)
Sn–C9	2.131(2)	O–Sn–N2	73.72(6)
Sn–N2	2.181(2)	C9–Sn–N2	173.66(7)
Sn–N1	2.227(2)	O–Sn–N1	146.87(6)
Sn–Cl2	2.469(1)	C9–Sn–N1	100.76(7)
Sn–Cl1	2.473(1)	N2–Sn–N1	73.17(6)
O–C8	1.293(2)	O–Sn–Cl2	88.73(5)
C1–C5	1.350(3)	C9–Sn–Cl2	94.24(7)
N2–C6	1.281(3)	N2–Sn–Cl2	83.72(5)
N2–N3	1.368(2)	N1–Sn–Cl2	86.71(5)
N3–C8	1.347(3)	O–Sn–Cl1	89.46(5)
C5–C6	1.480(3)	C9–Sn–Cl1	96.04(7)
		N2–Sn–Cl1	85.82(5)
		N1–Sn–Cl1	89.15(5)
		Cl2–Sn–Cl1	169.47(2)

The compound **1** crystallises with 1.5 molecules of water and the solvent plays a role in the packing as shown by the short distances between one of the oxygen atoms and N6 (3.06 Å) and between the two oxygens (2.66 Å) indicating possible H-bonds. Moreover, the complex molecule associates in a dimeric form with another molecule through the $N_4-H\cdots Cl1^{(i)}$ ($N_4\cdots Cl1^{(i)} = 3.40$ Å, N4–H–$Cl1^{(i)} = 149°$; (i) $= -x+1/2, -y+1/2, -z$) hydrogen bond. **2** crystallises with one ethanol and one disordered water molecule; while the water molecule shows no short contacts, the ethanol is involved in two hydrogen bonds, both as a donor ($O-H\cdots N6 = 2.906$ Å, O–H–N6 = 149°) and as an acceptor ($N_4-H\cdots O = 2.884$ Å, N4–H–O = 156°).

Fig. 3 shows an ORTEP diagram of **6**; Table 4 contains a selection of bond angles and distances for the same compound. The tin coordination is similar to that showed in the previously described complexes, with the ligand forming two strictly planar chelate rings. The distorted octahedron is completed by two axial chlorine atoms and the equatorial phenyl group. Distortion is clearly showed by bond angles around tin and it is not different from what has been observed in **1** and **2**. In this case the two chlorine atoms are much more symmetrically bonded to tin (Sn–Cl 2.469(1) and 2.473(1) Å, respectively). Sn–N1 and Sn–N2 distances are even shorter than those observed in **1** and **2**. The hydrazonic ligand has a high degree of planarity with the N4 amine group only 0.15 Å out of the mean plane. No solvent molecules are present; the crystal packing is mainly due to weak van der Waals interactions.

It is worth noting that **6** is one of the products of the reaction between Ph_2SnCl_2 and **Haps**; analogously, the reaction between the terdentate, monoprotic ligands, 2-pyridylketone 2-aminobenzoylhydrazone [21] or di-2-pyridylketone 2-thenoylhydrazone [22] and Ph_2SnCl_2 gave [PhSn(ligand-H)Cl_2] with the loss of benzene. The dearylation reaction is actively studied because it is involved in the intracellular degradation of organotin and organomercury derivatives [23] and it is, at least partially, responsible of the toxic effects of these compounds.

The complexes were characterised also by means of Mössbauer measurements. All the spectra present comparable hyperfine parameters (Table 5); therefore similar configurations in the solid state are assumed for all the compounds. The parameters, typical for monoorganotin derivatives in octahedral coordination [24], allow us to propose the coordination geometry obtained by X-ray diffraction for complexes **1**·1.5H_2O,

Table 5
Mössbauer data for the tin compounds

Compound	δ (mm s^{-1})	ΔE_Q (mm s^{-1})	Γ (mm s^{-1})	$A2/1$
1·2H_2O	1.18	1.82	0.79	1.12
2·C_2H_5OH	1.13	1.89	0.83	1.10
3	1.24	1.88	0.82	1.08
4	1.17	1.95	0.80	1.05
5·3H_2O	1.14	2.11	1.05	1.11
6·2.5H_2O	1.02	2.09	0.88	1.02

2·C_2H_5OH·H_2O, and **6**. The small values for the linewidth, in some case close to the theoretical one, are indicative for the presence of a single tin site in all the prepared compounds. The isomer shift decreases on replacing the butyl by the phenyl groups in the equatorial positions, reflecting the larger electron-releasing power of the alkyl group. The resulting increase in the electron density affects the imbalance in the electronic cloud around the tin nucleus. This effect results in a small increase in the quadrupole splitting values for compounds **1**·2H_2O compared to **2**·C_2H_5OH, and **3** compared to **4**. The **Haps** derivatives **5**·3H_2O and **6**·2.5H_2O are nearly insensitive to this substitution. The replacement in the ligand of a sulphur donor atom with the more electronegative oxygen, seems to be more efficient, at least under this aspect, than the substitution of the butyl group with the phenyl one; in fact the ΔE_Q value for the alkyl derivative, 2.11 mm s^{-1}, is somewhat higher than that for the aryl one, 2.08 mm s^{-1}. The presence of oxygen instead of sulphur as a donor atom is also indicated by a small decrease in the δ values for both the butyl and the phenyl derivatives. Calculations according to point charge formalism give results in full agreement with a *trans*-Cl,Cl configuration for all the compounds, while a *trans*-C,Cl arrangement should produce values that are too small.

4. Conclusions

The 2-pyridyl **H_2apt**, **Hapts** and **Haps** ligands react with monoorganotin species to give monometallic complexes, where the ligand results deprotonated and tridentate. The coordination around the metal is unequivocally determined by means of Mössbauer, ^{1}H-NMR and X-ray diffraction analysis: the two chlorines occupy the apical positions, while the ligand and the organic group lies in the equatorial plane. These complexes are promising from the biological point of view, because they contain organotin and, in the case of **1**–**4**, the C–S moieties, which have good antimicrobial activity.

5. Supplementary material

Crystallographic data for the structural analysis have been deposited with the Cambridge Crystallographic Data Centre, CCDC No. 151865, 151866 and 151867 for compounds **1**·1.5 H_2O, **2**·C_2H_5OH·H_2O and **6**, respectively. Copies of this information may be obtained free of charge from The Director, CCDC, 12 Union Road, Cambridge CB2 1EZ, UK (E-mail: deposit@ccdc.cam.ac.uk or www: http://www.ccdc.cam.ac.uk).

Acknowledgements

Thanks are due to the Centro di Studio per la Strutturistica Diffrattometrica del CNR and Centro Interfacoltà Misure "Giuseppe Casnati" of Parma for technical assistance.

References

[1] M. Carcelli, D. Delledonne, A. Fochi, G. Pelizzi, M.C. Rodríguez-Argüelles, U. Russo, J. Organomet. Chem. 544 (1997) 29.
[2] D.X. West, S.B. Padhye, P.B. Sonawane, Struct. Bonding 76 (1991) 1.
[3] T. Tunde Bamgboye, O.A. Bamgboye, Inorg. Chim. Acta 144 (1988) 249.
[4] R.S. Barbieri, H.O. Beraldo, C.A.L. Filgueiras, A. Abras, J.F. Nixon, P.B. Hitchcock, Inorg. Chim. Acta 206 (1993) 169.
[5] L. Labib, T.E. Khalil, M.F. Iskander, L.S. Refaat, Polyhedron 15 (1996) 349.
[6] J.S. Casas, M.S. García-Tasende, C. Maichle-Mössmer, M.C. Rodríguez-Argüelles, A. Sánchez, J. Sordo, A. Vázquez-López, S. Pinelli, P. Lunghi, R. Albertini, J. Inorg. Biochem. 62 (1996) 41.
[7] J.S. Casas, M.C. Rodríguez-Argüelles, U. Russo, A. Sánchez, J. Sordo, A. Vázquez-López, S. Pinelli, P. Lunghi, A. Bonati, R. Albertini, J. Inorg. Biochem. 69 (1998) 283.
[8] T.A. Blumenkopf, J. Harrington, C.S. Koble, D.D. Bankston, R.W. Morrison, E.C. Bigham, V.L. Styles, Th. Spector, J. Med. Chem. 35 (1992) 2306.
[9] B. Moubaraki, K. Murray, J.D. Ranford, J.J. Vittal, X. Wang, Y. Xu, J. Chem. Soc. Dalton Trans. (1999) 3573.
[10] A. Bacchi, M. Carcelli, P. Pelagatti, C. Pelizzi, G. Pelizzi, F. Zani, J. Inorg. Biochem. 75 (1999) 123.
[11] S. Ianelli, P. Mazza, M. Orcesi, C. Pelizzi, G. Pelizzi, F. Zani, J. Inorg. Biochem. 60 (1995) 89.
[12] A. Bacchi, A. Bonini, M. Carcelli, F. Ferraro, E. Leporati, C. Pelizzi, G. Pelizzi, J. Chem. Soc. Dalton Trans. (1996) 2699.
[13] N. Walker, D. Stuart, Acta Crystallogr. A 39 (1983) 158.
[14] SADABS, Area Detector Absorption Correction, Siemens Industrial Automation inc., Madison, WI, 1996.
[15] A. Altomare, G. Cascarano, C. Giacovazzo, A. Guagliardi, M.C. Burla, G. Polidori, M. Camalli, J. Appl. Crystallogr. 27 (1994) 435.
[16] G.M. Sheldrick, SHELXL97: Program for Structure Refinement, University of Gottingen, Germany, 1997.
[17] M. Nardelli, J. Appl. Crystallogr. 28 (1995) 659.
[18] L.J. Farrugia, J. Appl. Crystallogr. 30 (1997) 565.

[19] SAINT, Area Detector Integration Software, Siemens Industrial Automation inc., Madison, WI, 1995.
[20] J.S. Casas, M.V. Castaño, M.C. Rodríguez-Argüelles, A. Sánchez, J. Sordo, J. Chem. Soc. Dalton Trans. (1993) 1253.
[21] S. Ianelli, M. Orcesi, C. Pelizzi, G. Pelizzi, G. Predieri, J. Organomet. Chem. 451 (1993) 59.
[22] M. Carcelli, C. Pelizzi, G. Pelizzi, P. Mazza, F. Zani, J. Organomet. Chem. 488 (1995) 55.
[23] H. Strasdeit, A. von Dollen, W. Saak, M. Wilhelm, Angew. Chem. Int. Ed. Engl. 39 (2000) 784.
[24] R. Barbieri, F. Huber, L. Pellerito, G. Ruisi, A. Silvestri, in: P.J. Smith (Ed.), Chemistry of Tin, Blackie, Glasgow, 1997.